Properties of Palm Oil Ash Geopolymer Containing Alumina Powder and Field Para Rubber Latex

Abideng Hawa [1]*, Preecha Salaemae [1], Akkadath Abdulmatin [1],
Krittiya Ongwuttiwat [1], Woraphot Prachasearee [2]

[1] Infrastructure and Materials Innovation Research Unit, Department of Civil Engineering, Princess of Naradhiwas University, Narathiwat 96000, Thailand.

[2] Department of Civil Engineering, Prince of Songkla University, Songkhla 90110, Thailand.

Abstract

Most geopolymer binder is produced using raw materials comprising powder with high silica and alumina content. Additionally, fine aggregate is prepared with river sand for high bulk density. This research proposes using palm oil ash (POA) for the main binder and palm oil clinker (POC) for the fine aggregate. The chemical composition of POA has high levels of silica but low alumina, so it must undergo partial replacement with alumina powder (AP). POA and POC are waste by-products of electrical power plants. The properties to be investigated include compressive strength, bulk density, water absorption, and microstructure. The effect of mixture composition, i.e., POA and field Para rubber latex (FPRL), on those properties is of particular interest. POA was substituted by AP and FPRL at 2.5%, 5%, 7.5%, and 10%, and at 1%, 3%, 5%, and 10%, respectively. Geopolymer mortars were cured at ambient temperature for 24 hours and kept at ambient temperature until testing. The compressive strengths of the geopolymer mortars were tested at 1, 7, and 28 days. The results showed that the optimal mixture consisted of 5% AP in the case of AP only and 1% FPRL in the case of FPRL only, while the ternary optimal mixture of 1% FPRL and 7.5% AP achieved higher compressive strengths than the control (CT) sample at 28.16, 19.98, and 25.30 MPa, respectively, after 28 days of curing. Bulk density increased with the addition of AP and FPRL. The microstructures of the geopolymer samples investigated using SEM-EDX showed the presence of different elements with different mixtures and displayed a dense, compact geopolymer matrix with high compressive strength. Using large amounts of POA in combination with AP and FPRL improved the environmental aspects of landfill disposal.

Keywords: Alumina Powder; Field Para Rubber Latex; Palm Oil Ash; Palm Oil Clinker; Geopolymer.

1. Introduction

The construction industry is the largest user of natural resources for concrete materials, comprising 70% coarse and fine aggregates. Continuously increasing infrastructural construction requires large amounts of river sand to make fine aggregate. Considerable attempts have been made to find new materials and recycle waste materials to use instead of natural sand aggregates, thereby protecting the environment.

Using Ordinary Portland Cement (OPC) as a binder generates large amounts of carbon dioxide (CO_2) [1]. One potential replacement for OPC is using a geopolymer binder with similar mechanical properties. Many new geopolymer binder materials are still in the development stage to produce the reaction of an aluminosilicate with powder from

---

industrial waste. To date, geopolymers have been prepared using fly ash (FA) [2-4] and ground granulated blast furnace slag (GGBS) [5, 6]. Natural raw materials can be used to produce geopolymers such as metakaolin (MK) [7-9], pumice powder [10, 11] and red mud [12, 13]. These materials have major chemical compositions of SiO_2 and Al_2O_3 that greatly impact the geopolymerization process. Some agro-industry by-products include palm oil ash, rice husk ash, bagasse ash, wood ash, and Para wood ash with low Al_2O_3 content. These raw materials can be used as partial replacements for FA [14-16], GGBS [17] and MK [18-20] to make high strength geopolymer binders.

Palm oil ash (POA) and palm oil clinker (POC) are agro-waste produced and accumulated as biomass at power plants in southern Thailand. Normally, POA and POC waste is sent to landfills, resulting in an environmental problem with more than 280,000 tons of waste produced since 2011 [18]. POA can be classified as a pozzolanic material and can be used as a partial cement replacement [21] and a partial replacement of fly ash geopolymer [14, 22]. Nowadays, increased interest has been focused on POA, especially among researchers from countries with a large palm oil industry. Research into the utilization of POA as a geopolymer binder has been carried out [23]. It can be generally concluded that POA geopolymers have relatively low strength compared to fly ash geopolymers. This is a restriction resulting from the raw materials used for the geopolymer binder. The improvement of the geopolymer binder from POA should be the main focus of attention. Amri et al. [24] reported that graphene oxide could be used as an additive to improve the compressive strength of POA-based geopolymers. The increase in compressive strength was nearly double compared to geopolymers without graphene oxide. Meanwhile, Rattanasak et al. [25] found that the inclusion of aluminum hydroxide ($Al(OH)_3$) enhanced the geopolymerization process. Mijrash et al. [26] used POA to activate and produce geopolymer binders, while mixtures of alumina hydroxide, calcium hydroxide, and silica fume, in addition to the alkaline activator, have also been used to increase the efficiency of POA-based geopolymers. Geopolymer mortars can use POC for the replacement of normal sand for lower bulk density. Darvish et al. [27] showed that geopolymer mortars were prepared by POC aggregate. Results showed bulk densities ranging from 1,710-1,754 kg/m^3.

In its fresh or field state, FPRL also includes non-rubber content such as sludge, proteins, and some inorganic materials with about 30–40% rubber particles [28]. Generally, FPRL in Thailand has 20–45% rubber particles and 50–75% water and other materials [29]. In 2020, Thailand produced approximately 4,859,000 tons of Para rubber [30]. Therefore, the amount of FPRL produced annually in Thailand is of the order of 10.8–24.3 million tons. Normally, FPRL is mixed into normal concrete, but it has reduced strength. Research by Yaowarat et al. [31] involved the preparation of concrete with natural rubber latex. The results indicated that an increase in rubber reduced the compressive strength but could improve the flexural strength of some mixtures. In the case of geopolymers, Hawa and Prachasaree [2] reported that fly ash based geopolymers containing 1%, 2.5%, and 5% FPRL were heat cured at 80 ºC for 0.5, 1, 2, and 4 h. The results showed that heat curing for 4 hours determined high early strength, especially for geopolymer mortar with 1% FPRL.

In South East Asia, palm oil production by-products are alternative materials for aggregate concrete. The palm oil industry generates large amounts of dregs such as palm kernel shell, palm oil ash, and palm oil clinker (POC). POC has been studied for potential application as a sand replacement material. Kabir et al. [32] reported that POC could be used as aggregate to make geopolymer concrete with improved compressive strength because the porous POC aggregate increased the stiffness and improved the bond with mortar in the concrete.

2. Materials and Methods

2.1. Research Methodology

The methodology used in this research is summarized in the flowchart shown in Figure 1.

2.2. Materials

2.2.1. Palm oil ash

Palm oil ash (POA) obtained from burning palm kernel shells, empty fruit bunches, and mesocarp fiber was collected from an electrical power plant in Narathiwat Province in the south of Thailand. The raw palm oil ash (palm oil ash and palm oil clinker) was sieved through a 600 μm sieve to separate large pieces of palm oil clinker and incompletely combusted materials before grinding by a modified Los Angeles machine for 5 hours. The particle size distribution of the POA is shown in Figure 2, with the chemical composition of the POA by XRF test shown in Table 1. Major components of the POA were SiO_2, K_2O, and CaO at 56.84%, 8.60%, and 7.74%, respectively, which had a low amount of Al_2O_3.

Table 1. Chemical composition of POA and AP

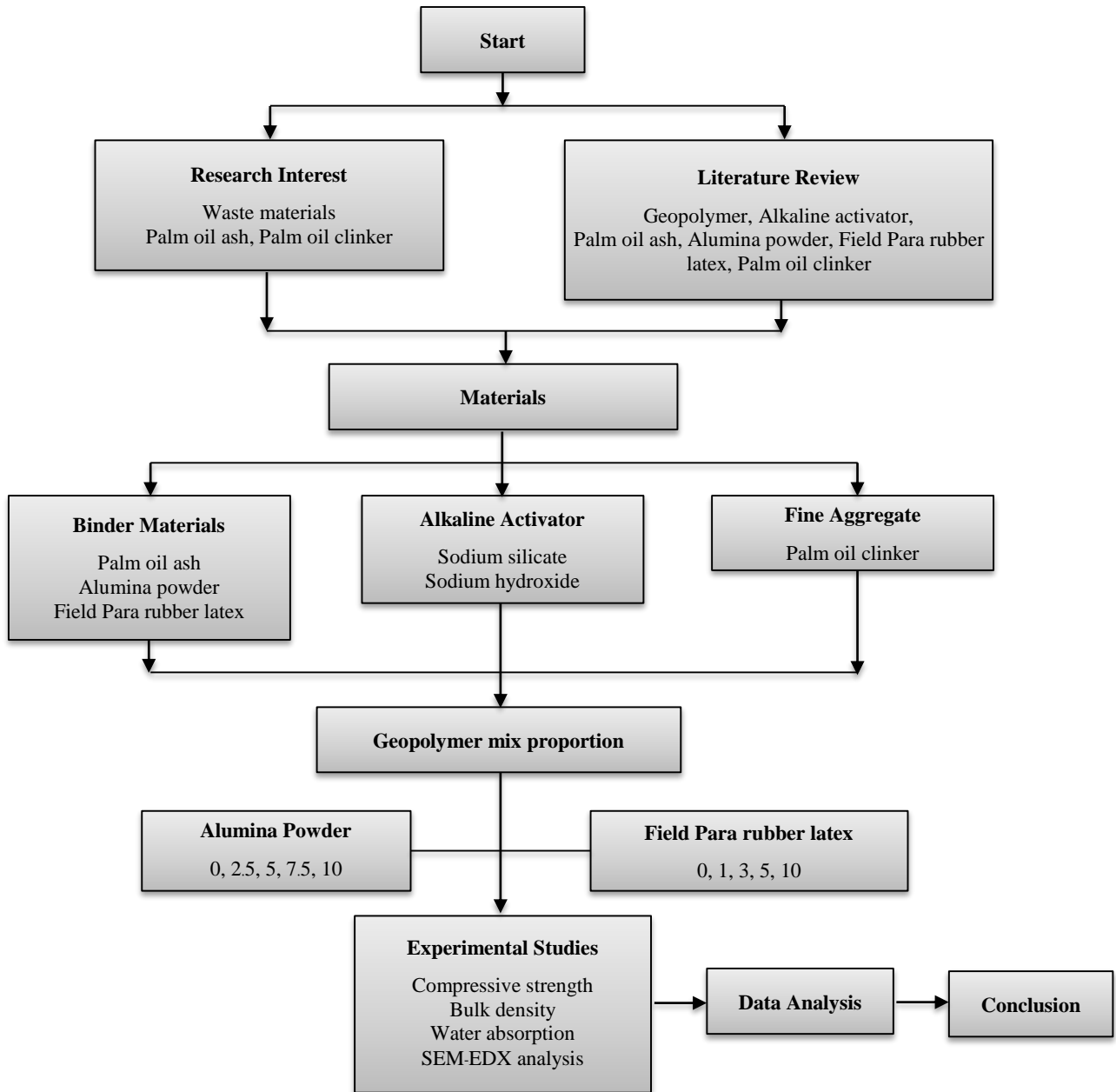| Materials	MgO	Al$_2$O$_3$	SiO$_2$	Fe$_2$O$_3$	P$_2$O$_5$	SO$_3$	K$_2$O	CaO	MnO	TiO$_2$
POA	6.54	1.06	56.84	2.46	6.96	1.92	8.60	7.74	0.21	-
AP	-	99.66	0.11	-	-	-	-	-	-	0.10

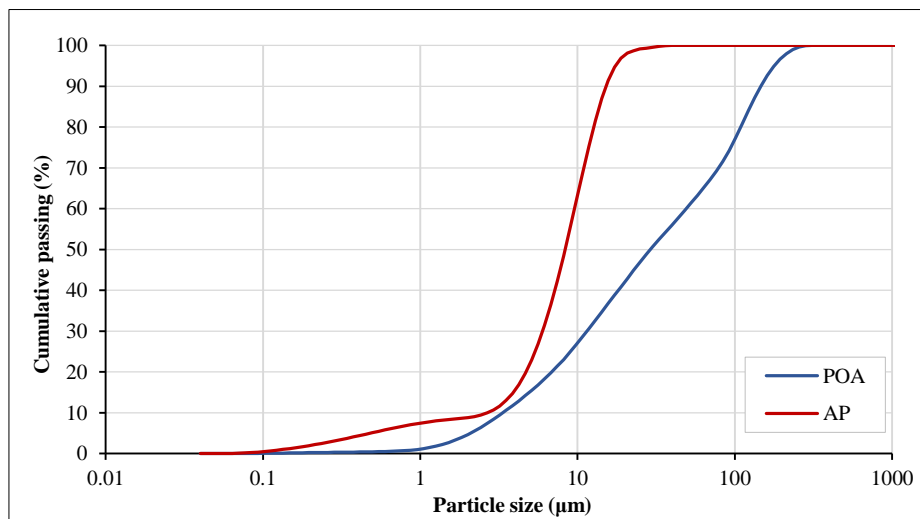**Figure 1. Flowchart of the research methodology**

Figure 2. Particle size distribution of POA and AP

The POA was ground into powder using a Los Angeles grinding machine and the particle morphology was investigated by scanning electron microscope (SEM). The crushed particles were mainly round with rough surfaces and some had angular shapes, as shown in Figure 3, with the XRD pattern shown in Figure 4. Major phases of quartz (SiO_2), cristobalite (SiO_2) and silicon (SiO_2) were detected. Substantial movement was also detected in the XRD profile from 17º to 35º (2θ) representing an amorphous phase [33].
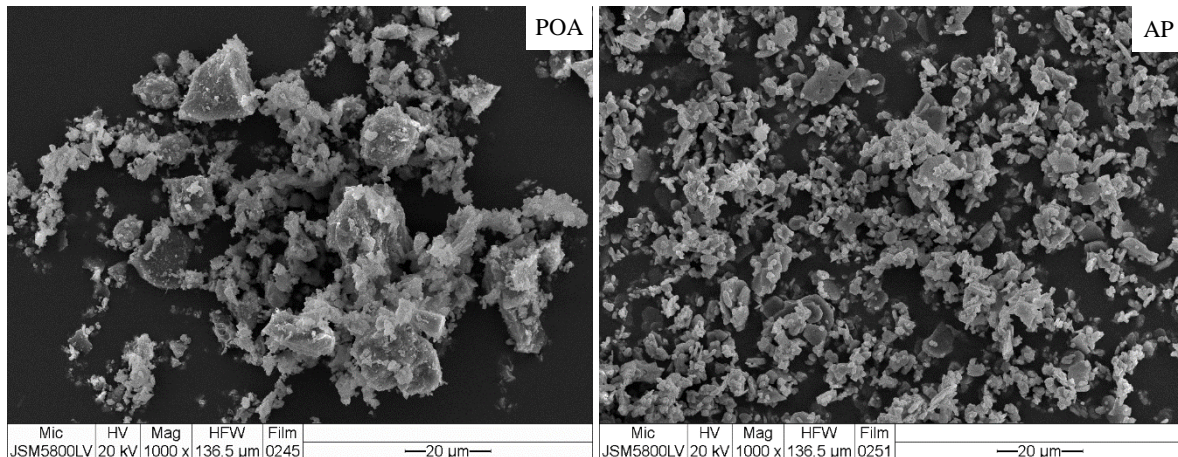

Figure 3. Particle morphologies of the ground POA and AP
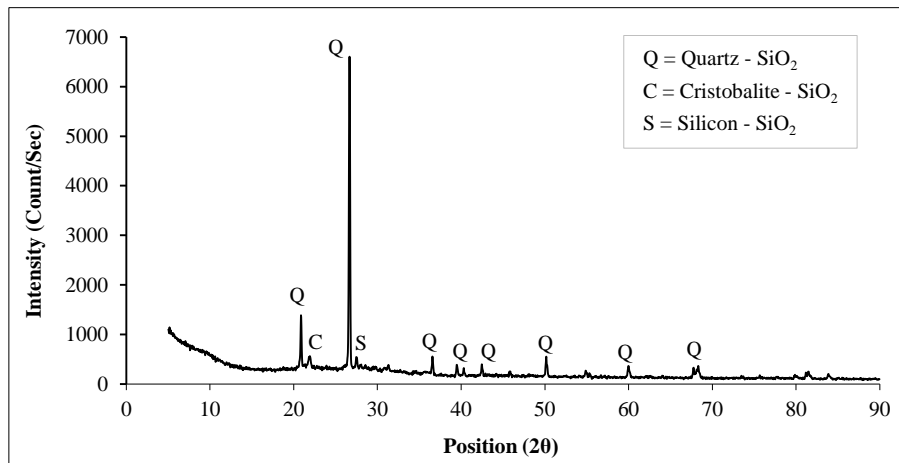

Figure 4. XRD patterns of POA

2.2.2. Alumina Powder

The alumina powder (AP) particle size distribution is shown in Figure 2. AP had a smaller size of 45 µm. Table 1 shows the chemical composition of AP with major Al_2O_3 content. Figure 5 shows the X-ray diffraction (XRD) pattern of AP with major phases of oxonium (Al_2O_3) and corundum ((H_3O)$_2Al_{22}O_{34}$) detected.
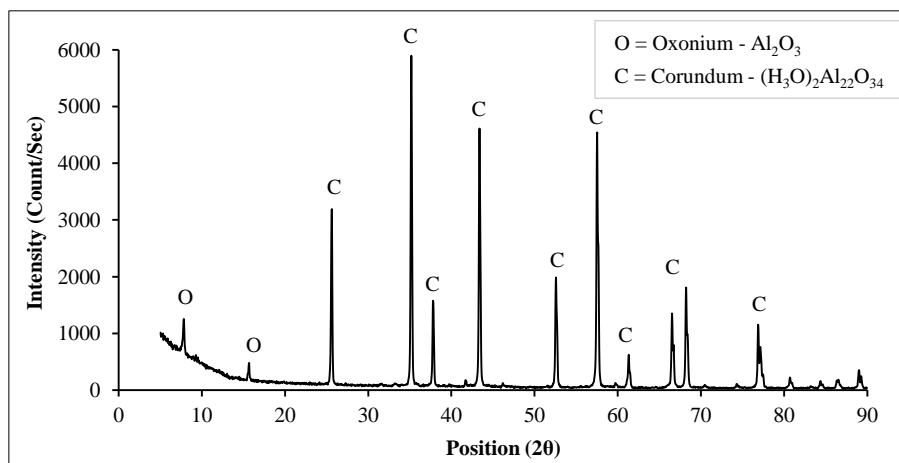

Figure 5. XRD pattern of AP

2.2.3. Field Para Rubber Latex

FPRL from the rubber tree clonal variety RRIM 600 was collected from Narathiwat Province, Southern Thailand. The particle size of FPRL solid content was in the range of 0.04-4.0 µm. FPRL is a suspension with 25-45% total solid content [29].

2.2.4. Alkaline Activator

Sodium silicate and sodium hydroxide at industrial grade with 99% purity were prepared as alkali activators. Sodium silicate solution was chosen with a chemical composition of 14.85 wt% Na_2O, 29.45 wt% SiO_2 and 55.70 wt% H_2O. The alkali activation solution was prepared by mixing sodium silicate (Na_2SiO_3) with sodium hydroxide (NaOH) within ratio at 2.5:1.

2.2.5. Palm Oil Clinker

Palm oil clinker (POC) is a by-product of electrical power plants resulting from the ignition of palm kernel shells, empty fruit bunches, and mesocarp fibers (Figure 6-a). The POC was crushed and sieved in the laboratory to obtain a particle size below 4.75 mm for use as fine aggregate. POC has a porous nature (Figure 6-b) and is lightweight with high water absorption. The strength and density of POC fulfill the structural lightweight concrete block and pavement requirements. The physical properties of POC are presented in Table 2. Sieve analysis was conducted in accordance with ASTM C136/C136M-19 [34]. Figure 7 shows the particle size distribution of POC based on ASTM C33/C33M-18 [35], falling in the well-graded fine aggregate category.
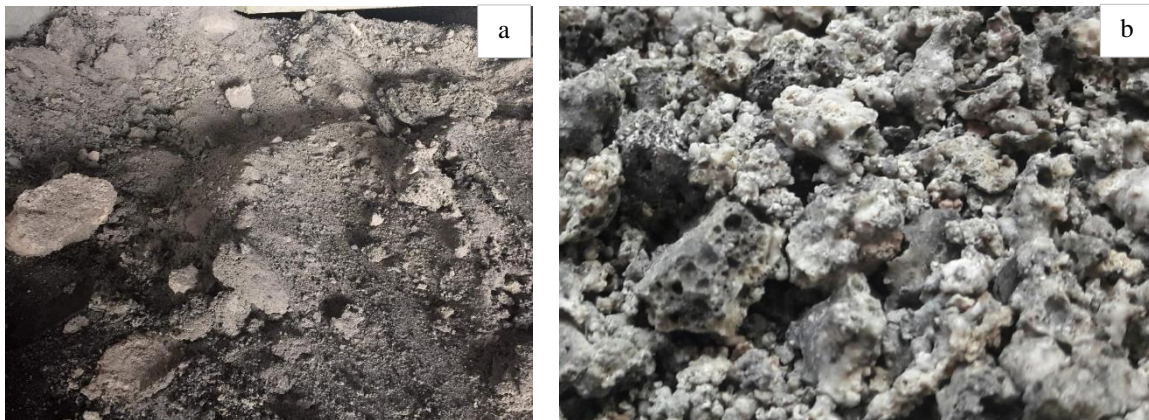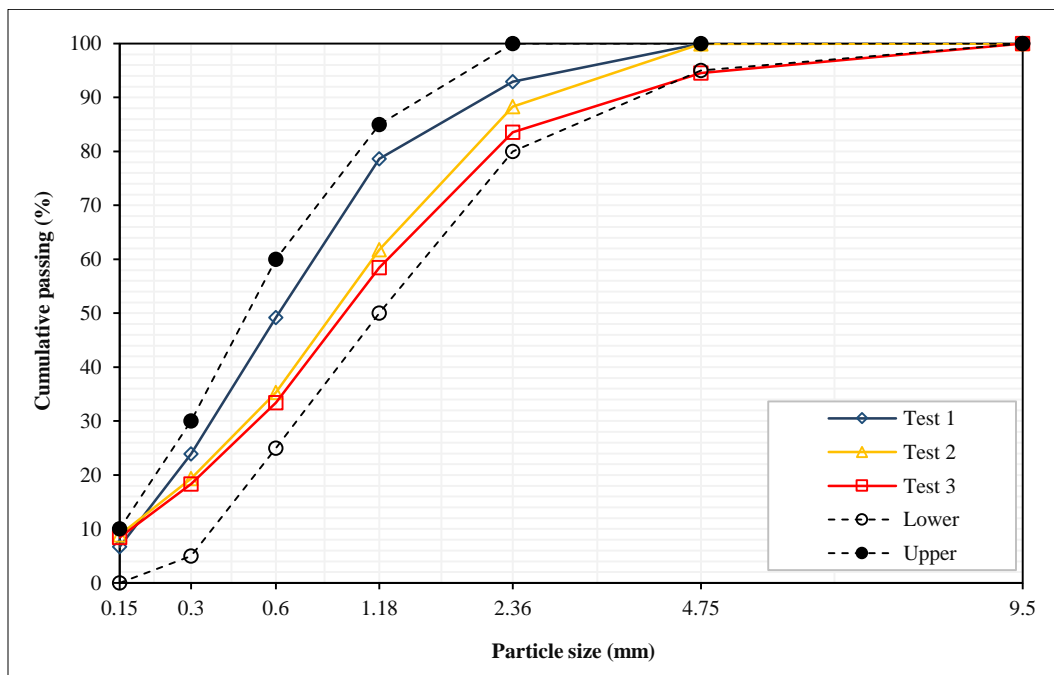

Figure 6. Physical properties of POC

Figure 7. Particle size distribution of POC

Table 2. Properties of palm oil clinker

Property	Unit	Value
Loose bulk density	kg/m^3	673
Compacted bulk density	kg/m^3	724
Bulk specific gravity)oven-dry(	-	1.83
Bulk specific gravity) SSD(	-	1.91
Apparent specific gravity	-	1.98
Absorption	%	4.09
Fineness modulus		2.6-3.0

2.3. Preparation and Mixture Proportions

A total of 25 mixture ingredients were prepared, as shown in Table 3, with binder materials (POA, AP and FPRL), sodium silicate, sodium hydroxide, water, and POC aggregate. Geopolymer samples were designed and investigated for partial POA replacement by AP and FPRL. The factors in the experimental design led to 25 different formulations. This is full factorial for AP (2.5, 5, 7.5, and 10% by wt.) and FPRL (1, 3, 5, and 10% by wt.). The mass ratio of binder: activator: POC: water was 1:0.6:2.75:0.5. Sodium hydroxide flakes were mixed with sodium silicate liquid by weight proportion of 1:2.5 for an alkali solution. The geopolymer mortar was mixed in four steps. Step 1, binder (POA+AP) and POC were mixed by hand for about 3 minutes. Step 2, NaOH and Na2SiO3 were mixed into a homogeneous alkaline solution and water was added. Step 3, binder materials and POC aggregate were mixed with the alkaline solution. Step 4, geopolymer slurries were added with FPRL and mixed for about 5 minutes. The alkaline activator in step 2 had an exothermic reaction conducive to fast setting [18, 36]. After mixing, the geopolymer slurries were poured into acrylic 50 mm cube molds to set and form samples for compressive strength testing and were compacted in accordance with ASTM C109/C109M-16 [37]. The geopolymer mortars in the acrylic molds were cured at ambient temperature for 24 h. The samples were then demolded and stored at an ambient temperature of 30±2 °C until testing. Compressive strength testing of the geopolymer mortars was conducted at 1, 7, and 28 days.

Table 3. Mixture proportions of geopolymer mortar (by weight)

Symbol	POA (g)	AP (g)	FPRL (g)	Sodium silicate (g)	Sodium hydroxide (g)	POC (g)	Water (g)
CT	100	-	-	42.85	17.15	275	50
2.5A	97.5	2.5	-	42.85	17.15	275	50
5A	95	5	-	42.85	17.15	275	50
7.5A	92.5	7.5	-	42.85	17.15	275	50
10A	90	10	-	42.85	17.15	275	50
1L	99	-	1	42.85	17.15	275	50
1L2.5A	96.5	2.5	1	42.85	17.15	275	50
1L5A	94	5	1	42.85	17.15	275	50
1L7.5A	91.5	7.5	1	42.85	17.15	275	50
1L10A	89	10	1	42.85	17.15	275	50
3L	97	-	3	42.85	17.15	275	50
3L2.5A	94.5	2.5	3	42.85	17.15	275	50
3L5A	92	5	3	42.85	17.15	275	50
3L7.5A	89.5	7.5	3	42.85	17.15	275	50
3L10A	87	10	3	42.85	17.15	275	50
5L	95	-	5	42.85	17.15	275	50
5L2.5A	92.5	2.5	5	42.85	17.15	275	50
5L5A	90	5	5	42.85	17.15	275	50
5L7.5A	87.5	7.5	5	42.85	17.15	275	50
5L10A	85	10	5	42.85	17.15	275	50
10L	90	-	10	42.85	17.15	275	50
10L2.5A	87.5	2.5	10	42.85	17.15	275	50
10L5A	85	5	10	42.85	17.15	275	50
10L7.5A	82.5	7.5	10	42.85	17.15	275	50
10L10A	80	10	10	42.85	17.15	275	50

2.4. Experimental Program

2.4.1. Testing Specimens

In this study, cubic samples with 50×50×50 mm dimensions were prepared for each of the geopolymer mortars to determine the compressive strength at the ages of 1, 7, and 28 days. After casting, the specimens were kept in their molds for 24 h at an average ambient temperature of 30±2 ℃, and were demolded and stored at ambient temperature until testing. The compressive strength of the samples was tested using a Universal Testing Machine (UTM) with a maximum capacity of 600 kN in accordance with the ASTM C109/C109M-16 [37].

The bulk density of the test samples of size 50×50×50 mm was measured after curing for 28 days. The mass of three samples was recorded and then divided by the volume of each sample to determine the average bulk density for three specimens. The bulk density was calculated using formula shown below (Equation 1):

$$\rho = \frac{M}{V} \tag{1}$$

where ρ is the bulk density, M is the mass of the sample (kg) and V is its volume (m^3).

The water absorption test measures the change in the mass of the saturated sample when allowing it to absorb water. In this study, after the geopolymer mortars were stored at ambient temperature (30±2 ℃) for 28 days, the geopolymer mortars were submerged in water. The samples were removed from water after 24 h and weight recordings were taken after drying the surfaces. The water absorption was calculated using the formula shown below (Equation 2):

$$W_{ab}(\%) = \frac{W_{ss} - W_{28}}{W_{28}} \times 100 \tag{2}$$

where W_{ab} is the water absorption, W_{ss} is the weight of the saturated surface of the sample (g) and W_{28} is the weight of the sample at 28 days (g).

2.4.2. SEM-EDX Analysis

Energy-dispersive X-ray (EDX) spectroscopy is an analytical technique that allows the chemical characterization/elemental analysis of materials. SEM-EDX tests were performed to analyze the matrices and elemental composition of geopolymer mortars using electron micrographs with small scraps of the samples after testing compressive strength. The samples were prepared by sputter coating with gold. Fracture surfaces of the matrices of geopolymer samples after the geopolymerization process were characterized by SEM-EDX. The specification of EDX was a QUANTA 400 model.

3. Results and Discussion

3.1. Compressive Strength

3.1.1. Effect of Alumina Powder

The source material (POA) had significantly high SiO$_2$ (56.84%), low Al$_2$O$_3$ (1.06%), and low CaO (7.74%). Consequently, the addition of alumina powder (AP) contributed Al2O3 content, leading to an increase in total Al$_2$O$_3$ in each mixture.

The increase in compressive strength of all geopolymer mortar mixtures with curing time with partial replacement of AP is shown in Figure 8. The compressive strength of the samples was dependent on the added AP amount and the curing time. In the control (CT) sample with only POA, compressive strength increased from 3.62 MPa at 1 day of curing to 18.86 MPa at 28 days. A similar phenomenon was presented by Ranjbar et al. [38] who found that geopolymer mortar from POA powder only (ET8 sample) had similar compressive strength for 28 days. It showed the lowest compressive strength in comparison with geopolymer containing fly ash. In the present research, the compressive strength of 18.86 MPa was obtained at 28 days, which may serve to testify that POA can be explained as a reactive material contributing effectively to reaction development. The activity of the alkali activator solution mixing with POA may correspond to the ability of the ash to transition from a slurry to a hard sample. However, the compressive strength values are under POC aggregate conditions. Previously, in a study by Islam et al. [39], geopolymer was prepared from 100% POA, and the maximum strength of 18 MPa achieved at 28 days occurred with 65 ℃ for 24 h oven curing and a sodium silicate to sodium hydroxide ratio of 2.49. The compressive strengths of all mixtures were similar on day 1. However, at 28 days, the mixtures had different compressive strengths as a result of different geopolymer process reactions. In the 5A sample with POA substituted at 5% AP, compressive strength was 5.19 MPa on day 1, and increased to 28.16 MPa after 28 days with only a small increase after 7 days. The POA substituted with AP showed higher strength compared to the sample without AP at 28 days because the Al$_2$O$_3$ from AP increased the ratio of SiO$_2$/Al$_2$O$_3$. The Al component tends to dissolve more easily than the Si components, and this enables a higher rate of condensation between silicate and aluminate species than the condensation between just silicate species [40]. Mijarsh et al. [26] reported that

palm oil fuel ash-based geopolymer containing $Al(OH)_3$ played an important role in the gel structure development of the geopolymer reaction and matrix strengthening. However, substitution of POA with AP up to 7.5% reduced the compressive strength of the geopolymer samples.
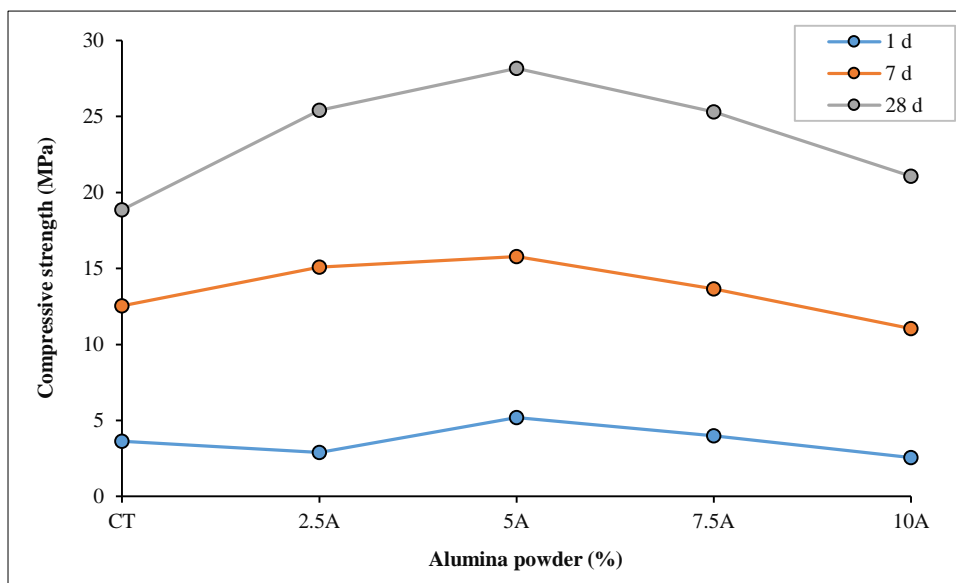

Figure 8. Compressive strength of geopolymer mortars containing AP

3.1.2. Effect of Field Para Rubber Latex

The compressive strengths of geopolymer samples after curing at ambient temperature for 24 h are shown in Figure 9. Development of the compressive strength of the CT, 1L, 3L, 5L, and 10L samples was compared at various FPRL values. The compressive strength after 1 day of curing was low but increased after 7 days. Samples cured at ambient temperature did not show accelerated geopolymerization compared with heat curing.
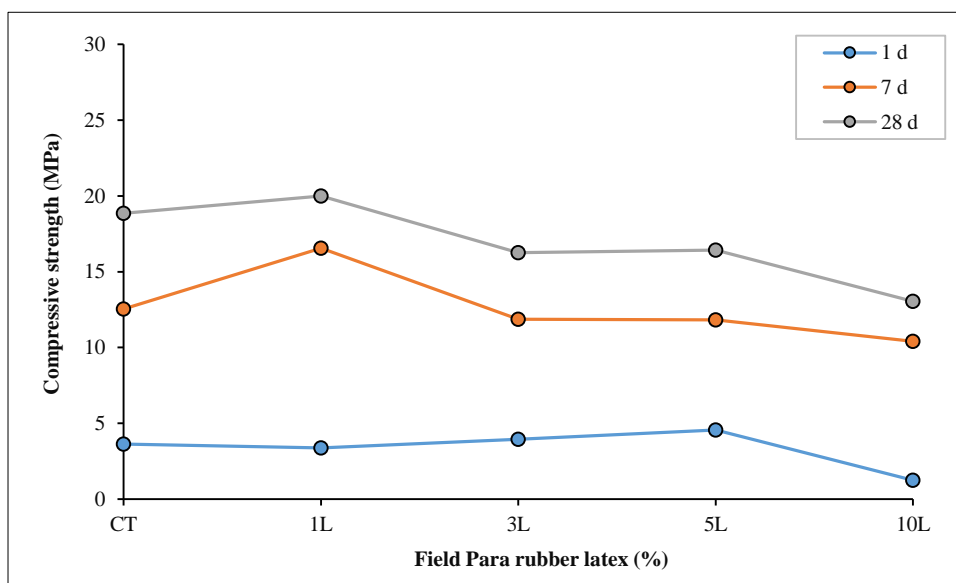

Figure 9. The compressive strength of geopolymer mortars

The compressive strength of POA geopolymers containing PFRL (Figure 9) decreased with increasing FPRL content due to dilution by water in the FPRL; more FPRL gave higher water content in geopolymer matrix. Kwek et al. [41] reported that POA geopolymer with increased liquid-to-solid ratio gave reduced compressive strength, while Salih et al. [42] used two values to investigate the effect of liquid-to-solid ratio on POA geopolymers. Results showed that high liquid content was attributed to low compressive strength due to voids in the matrix. Moreover, the investigation of geopolymers with FPRL by SEM showed that the matrix surface had large pores when increasing FPRL content [2, 43]. However, the 1L gave the highest compressive strength. This increased compressive strength was attributable to the structure of the geopolymer, which had a dense, compact matrix and contained fewer unreacted raw materials. In similar

research, Hawa et al. [2] investigated geopolymers prepared from fly ash containing FPRL of 1%, 2.5%, and 5% and various heat curing periods at 80 ℃ for 0.5, 1, 2, and 4 h. The results showed that geopolymer mortars with 1% FPRL had the highest compressive strength at 28 days. Meanwhile, Rath et al. [44] found that geopolymer concrete containing natural rubber latex exhibited increased compressive strength with 2% natural rubber latex. The 2% addition of latex in geopolymer concrete partially filled up voids and formed a porous coating on the surface of oxides of cementitious particles as well as aggregate particles.

3.1.3. Effect of Ternary Mortar Mixtures

Figure 10a-d show the values of compressive strength of geopolymer at 1, 7 and 28 days of ambient curing and the effect of the incorporation of the POA, FPRL and AP as the binder of geopolymer matrix. Compressive strengths on day 1 were similar. The samples were replaced with high volume binder (AP and FPRL) up to 5% and 10% FPRL. Compressive strength of 1% FPRL content decreased when mixing AP in the matrix (Figure 10a). The 1L7.5A sample gave higher compressive strength at 28 days than the other ternary mixture samples as the optimal content for POA geopolymer with FPRL and AP, while the sample with 1% FPRL had the highest compressive strength with FPRL only. The addition of 7.5% and 10% AP increased the compressive strength compared with the CT sample, showing that fresh geopolymer mortar had a good consistency. Samples with 1% FPRL mixed with 7.5% and 10% AP had a good effect on compressive strength when compared with geopolymer from POA only (CT sample). The addition of 7.5% and 10% AP reduced the consistency of fresh geopolymer mortars, while the addition of FPRL gave higher consistency than POA because of the water content in FPRL.
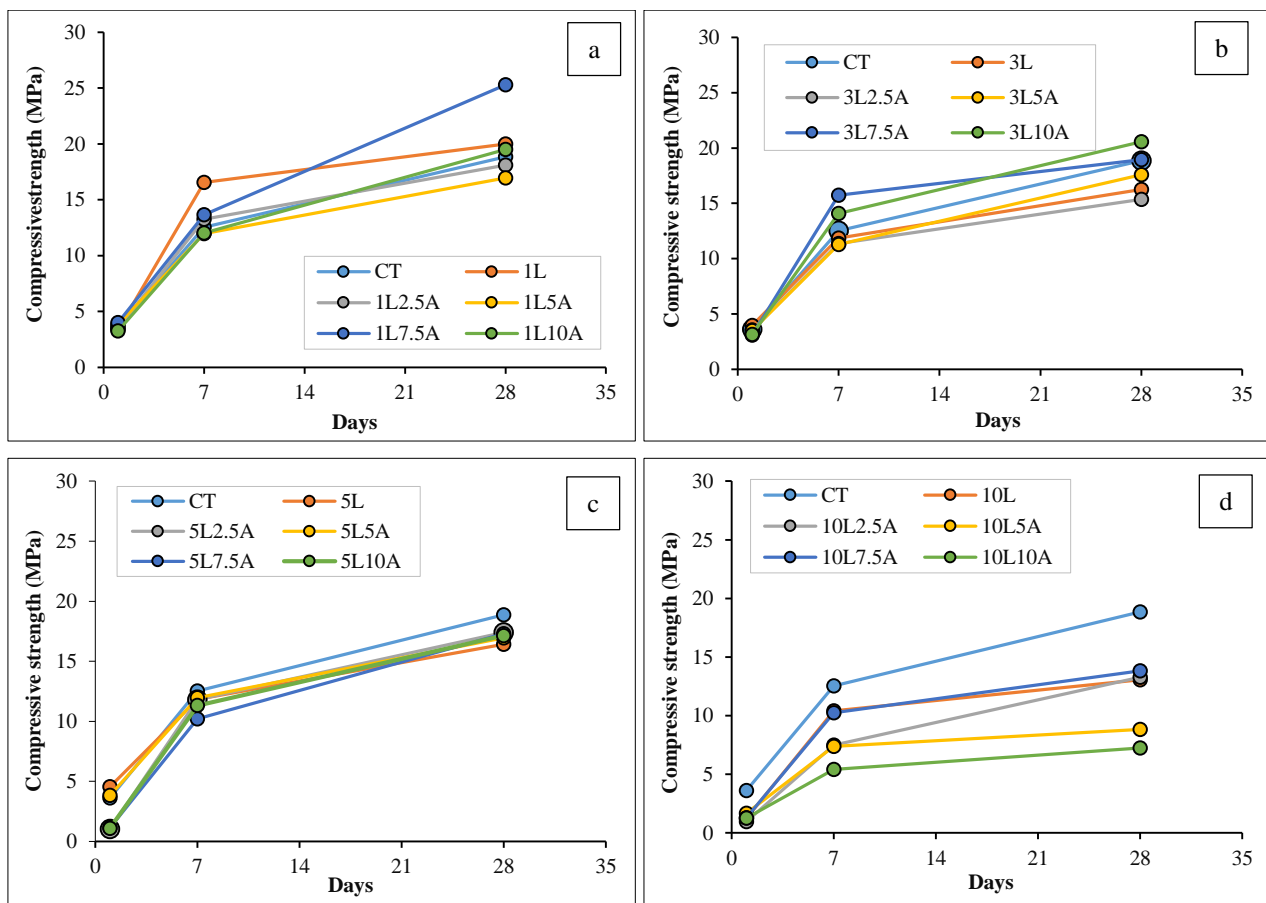

Figure 10. Compressive strength of geopolymer mortars containing FPRL and AP (a) 1% FPRL (b) 3% FPRL (c) 5% FPRL and (d) 10% FPRL

3.2. Bulk Density

Bulk densities of POA geopolymer mortars after curing at ambient temperature for 28 days with different AP ratios are illustrated in Figure 11-a. The results showed a significant effect of AP addition on the bulk density of POA geopolymer mortars, with bulk density increasing with higher AP content, ranging from 1,636 to 1,923 kg/m^3 when adding AP or FPRL to POC. The geopolymer matrix bulk density of the samples increased by 17.5% with the addition of 2.5% AP, while adding 5% and 7.5% AP increased bulk density by 14.1% and 13.8%, respectively. High differences in bulk density were mainly derived from the homogenous matrix and compact density compared to the pure POA geopolymer as the effect of a good geopolymerization process. The 10A sample showed small differences in bulk density

compared with the CT sample. Results of higher bulk density matched the high compressive strength of geopolymers with 2.5%, 5%, and 7.5% AP.
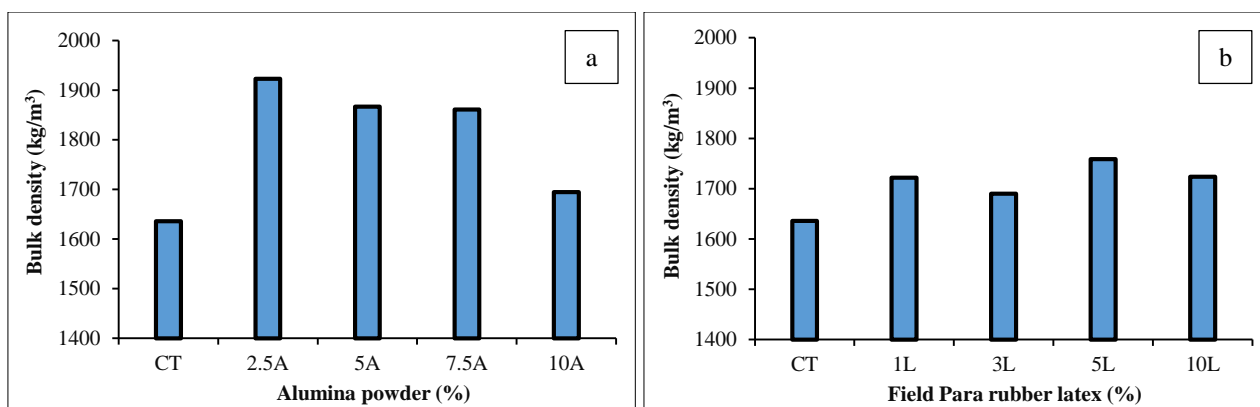

Figure 11. Effect of AP on bulk density of geopolymer mortars at 28 days, (a) AP and (b) FPRL

Results in Figure 11-b show that the bulk density of geopolymer mortars increased when samples were mixed with FPRL because the geopolymer using POC was extremely porous. FPRL is a liquid and entered the pores of POC. Hawa et al. [43] reported that an increase in FPRL reduced the bulk density as FPRL had lower specific gravity than fly ash. For research, the geopolymers were made from river sand with fine aggregate and a high volume of FPRL. Darvish et al. [27] reported that geopolymers made using POC aggregate showed bulk density at 28 days comparable with the respective NaOH molarity of the mixes. Bulk density values ranged from 1,710 to 1,754 kg/m^3, while geopolymers made with river sand gave bulk density at 28 days of 2,077 kg/m^3.

3.3. Water Absorption

Water absorption percentages of POA geopolymer mortars containing AP are presented in Figure 12-a. The results showed that the 24 h water absorption values varied between 0.67 and 2.13%. Water absorption of the geopolymer samples decreased with an increase in AP because the small AP particles were inserted in the POC pores. The 2.5A and 5A samples had significantly higher water absorption than the CT sample. The binder containing AP had lower volume, as AP had higher specific gravity than POA. Thus, free water in the geopolymer matrix was higher compared with the geopolymer without AP. In the geopolymerization process using liquids (sodium silicate, sodium hydroxide, and water), water was used more than the other liquids. Water absorption was tested at 28 days which had not been heated or oven-dried at 105 ± 5 ℃. This may explain the reason for the higher water absorption in 2.5A and 5A compared with the other samples. All the mixes had low absorption characteristics due to using powder and the results were influenced by binder type. Kabir et al. [32] used palm oil clinker for aggregate in geopolymer concrete. Results showed that water absorption values varied between 7.10 and 10.84% at 72 h after oven drying at 105 ± 5 ℃. Water absorption of POC aggregate was 6.08% for 5 to 9 mm and 5.56% for 9 to 14 mm.
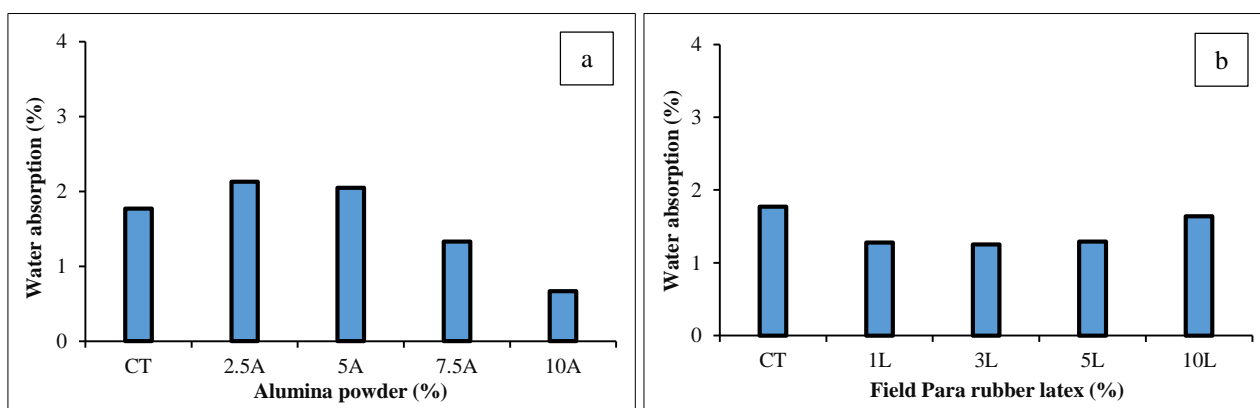

Figure 12. Percentage of water absorption in geopolymer mortars, (a) containing AP and (b) containing FPRL

Water absorption was measured to investigate the effect of FPRL content on geopolymer mortars cured at ambient temperature (Figure 12-b). Water absorption decreased with an increase in FPRL contents due to water in FPRL contributing free water in the geopolymer matrix. This trend was similar to the findings of Rath et al. [45], where geopolymer concrete mixed with rubber latex exhibited decreased water absorption. It can be concluded that rubber

latex at a higher percentage seals the pores on the surface of the samples to prevent water from entering inside. However, when geopolymer samples were replaced with 10% FPRL (10L sample), higher water absorption was recorded than for the 1L, 3L and 5L samples because of the addition of high FPRL with flakes and large pores. Investigation of the microstructure using SEM showed that geopolymers containing high volumes of FPRL had large pores [27]. Thus, water absorption of the mixture increased.

3.4. Microstructural Analysis

3.4.1. SEM-EDX Surface Characteristics of Geopolymer with AP

The surface and elemental distributions of POA geopolymer mortars containing AP at 5% and 10% are shown in Figures 13 and 14, respectively, and without AP are shown in Figure 15. Products from geopolymerization showed high values of oxygen, carbon, silica, sodium, potassium, calcium, aluminum, and magnesium. The chemical composition of POA is presented in Table 1. SEM images in Figure 15 showed that a few unreacted raw materials were covered with flakes on the nonhomogeneous CT sample surfaces, with POA having a round shape. For geopolymerization, the alkali solution reacted at the surface and leached the POA, with some unreacted POA from the geopolymerization also visible.
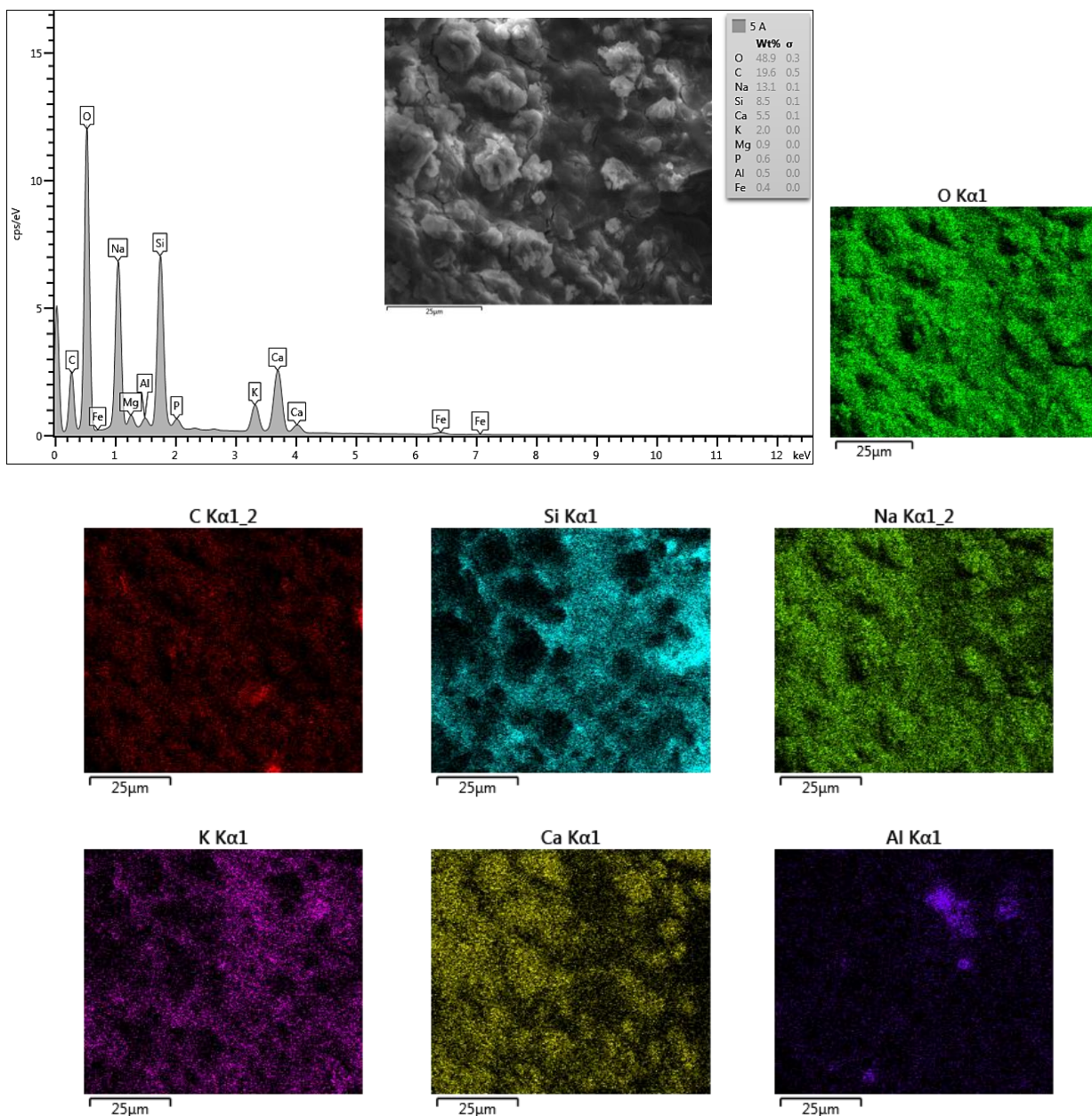

Figure 13. Texture and elemental distribution at the geopolymer 5A sample surface
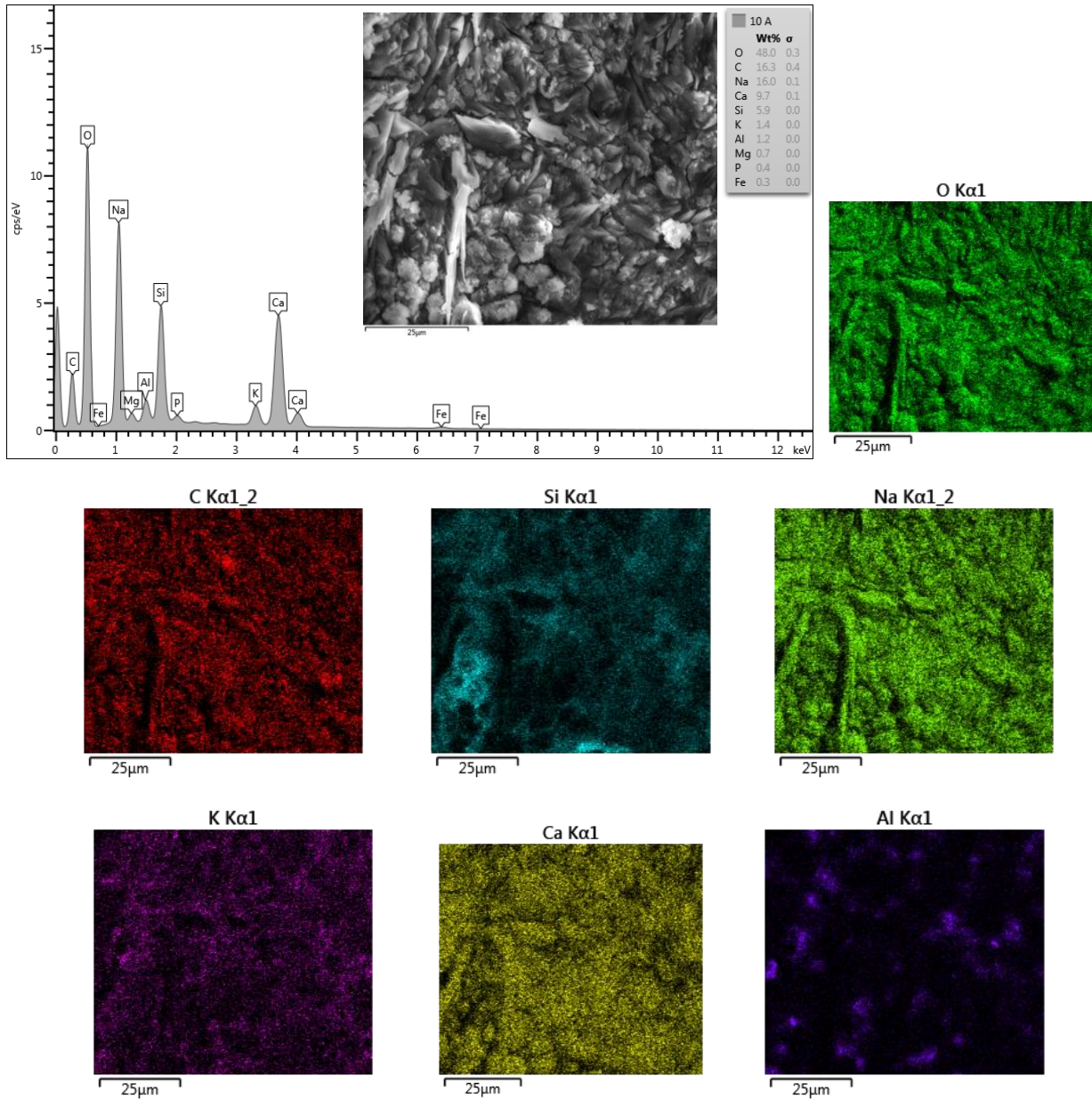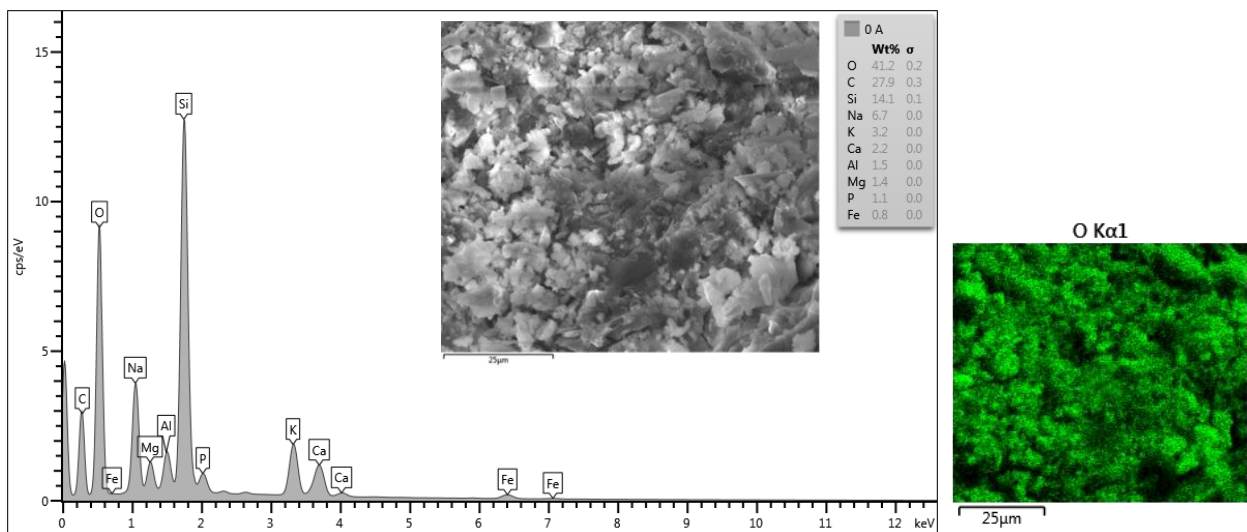
Figure 14. Texture and elemental distribution at the geopolymer 10A sample surface
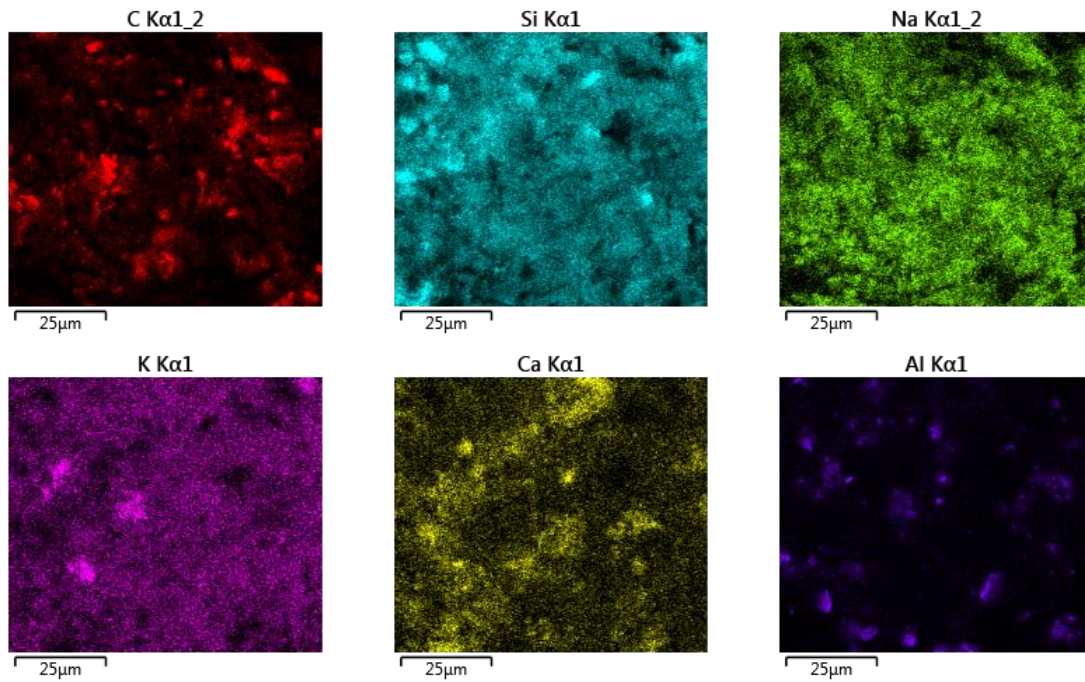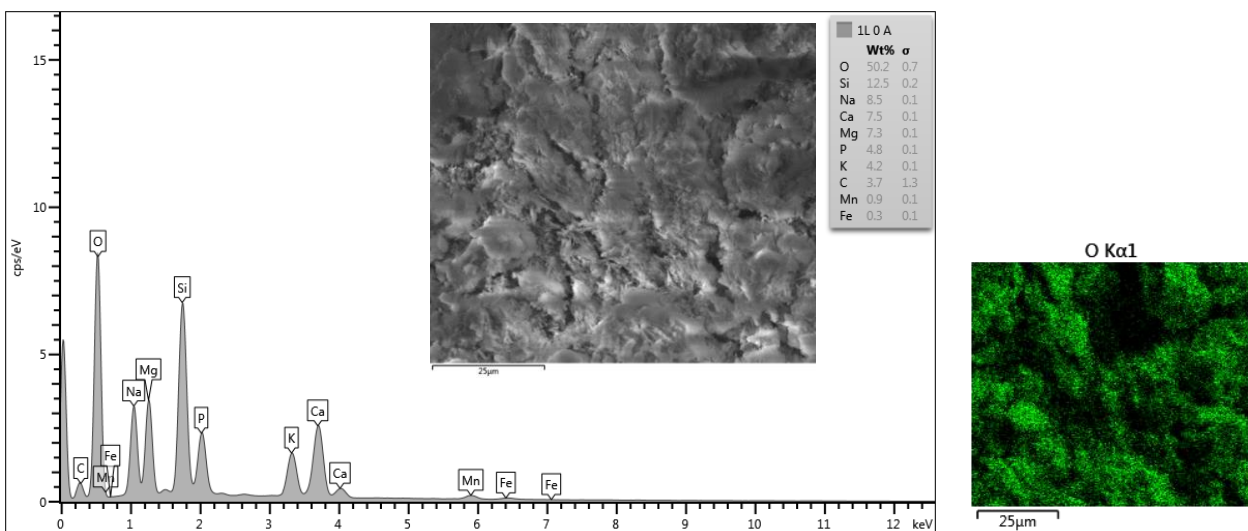
Figure 15. Texture and elemental distribution at the geopolymer CT sample surface

Figure 13 shows the typical microstructures of geopolymerization products obtained from this investigation. When comparing microstructures, the CT, 5A, and 10A samples revealed unreacted POA with flakes formed on the crust of the CT sample. The geopolymer products in the 10A sample were not linked on the matrices (Figure 15), while in the 5A samples, a lower proportion of unreacted POA was detected. The 5A samples had high homogeneity compared with the CT and 10A samples, while the compressive strength of the 5A specimens was higher than the CT and 10A samples, as presented in Figure 8.

3.4.2. SEM-EDX Surface Characteristics of Geopolymer with FPRL

Figures 16 and 17 show the microstructure of POA geopolymers containing FPRL that reacted with the alkaline activator after curing for 28 days at ambient temperature. Figure16 shows the rigorous formation of the geopolymer matrix with 1% FPRL that filled the voids among the geopolymer products, explaining why the compressive strength results displayed that the POA geopolymer containing 1% FPRL achieved higher strength at 28 days after curing compared with the 10L sample. The 1L sample, as the geopolymer matrix with aluminosilicate gel (geopolymer products), was densely compacted with a highly interconnected microstructure framework. However, for the 10L sample, Figure 17 shows microcracks on the surface matrix, thereby explaining the reduced compressive strength.
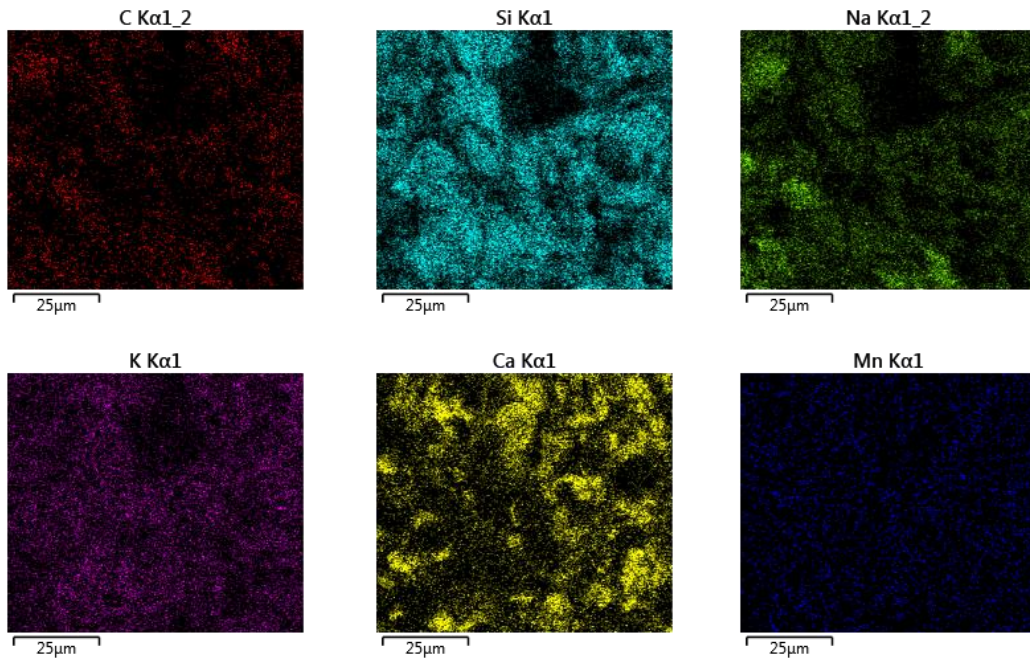
Figure 16. Texture and elemental distribution at the surface of geopolymer 1L sample
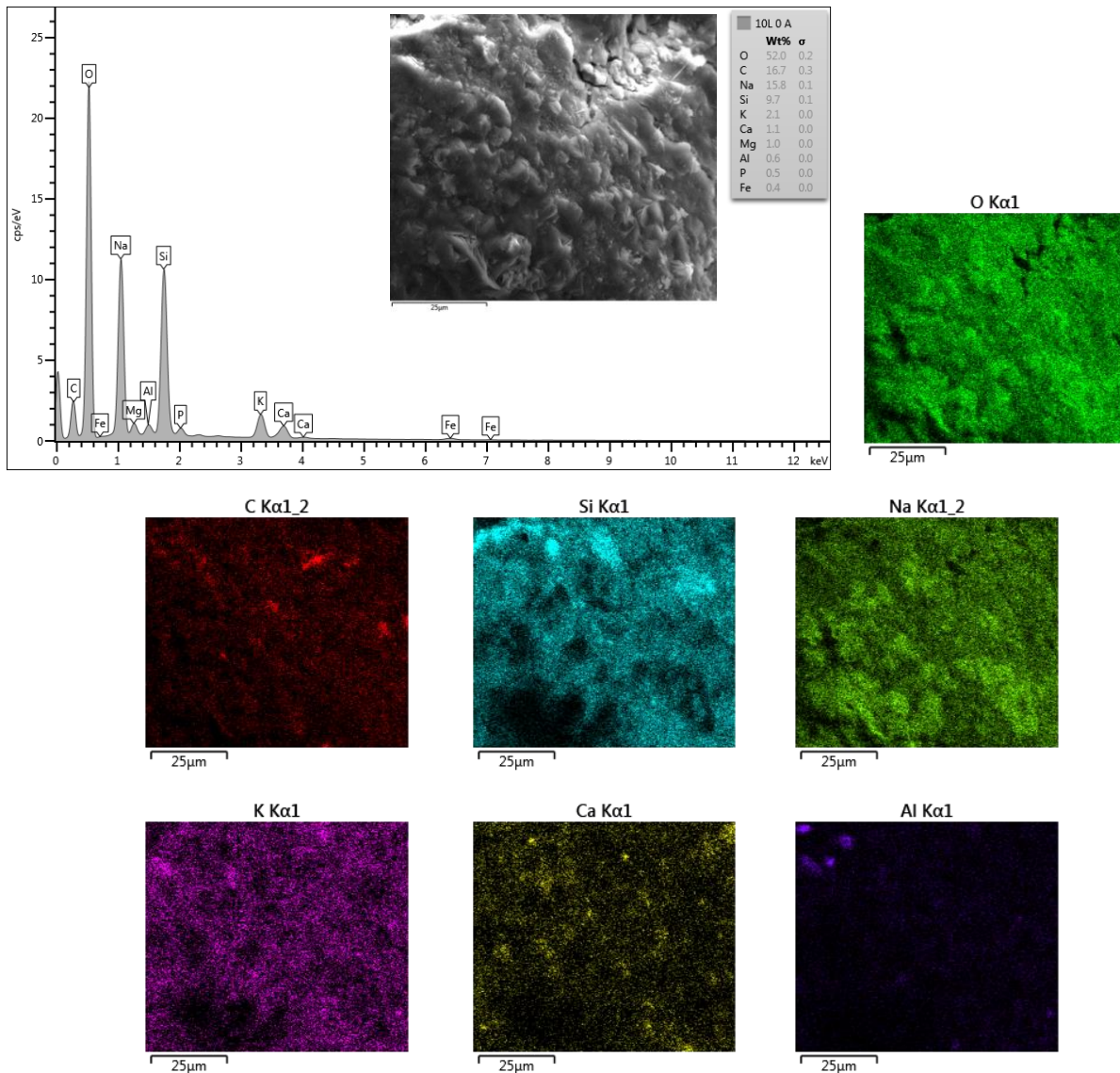

Figure 17. Texture and elemental distribution at the surface of geopolymer 10L sample

The EDX results displayed different components in the final products of POA geopolymer containing FPRL, while the POA geopolymer sample contained Si at 14.1%, and higher than the 1L and 10L samples because an increase in FPRL caused reduced POA and reduced Si elements, as POA had a high silica content. The Si/Ca ratios obtained from the EDX results for the CT sample were 6.41 and 1.67 for 1L and 8.82 for 10L, with the ratio of these elements closely related to the composition of C-S-H gel [39].

The sample mixtures showed the existence of sodium, attributed to the alkali activator solution, where it is the main element [46]. Si was also detected in all mixtures as present in the main binder (POA). Increased AP or FPRL reduced the Si content of the geopolymer matrix (Table 4). Based on the concentrations of the elements, the Si/Al ratios were 9.4, 5.7, 4.9, and 16.2 for CT, 5A, 10A, and 10L, respectively. He et al. [47] suggested that an increase in the Si/Al ratio improved product strength since more Si-O-Si bonds occurred, while Mijarsh et al. [26] and Arifin et al. [48] reported that high calcium and silicate with low aluminum encouraged the formation of calcium silicate hydrate (C-S-H) with higher amounts of aluminum, creating calcium alumina silicate hydrate (C-A-S-H) products that have excellent mechanical properties [49]. Salih et al. [50] reported that POA geopolymers produced C-S-H gel instead of aluminum silicate hydrate (A-S-H) gel due to the low alumina (Al) content. Geopolymer matrices with increased Ca content encouraged the formation of C-(N)-(A)-S-H gel, while decreased Ca content and increased Al and Si content encouraged the formation of N-A-S-H gel in the reaction products [51]. Highly interlinked Si-O-Si and Si-O-Al bonds constituted the network of N-A-S-H, with sodium and water molecules located in the skeleton. In the alumino silicate skeleton, the nature of the high geopolymerization process and extreme stability underlie the stability of N-A-S-H [52]. Thus, the enhanced strength of 5A was attributed to N-A-S-H gel. For 1% FPRL samples, the nonreacted FPRL acted as a filler in the geopolymer matrix and enhanced the mechanical properties.

Table 4. Elemental composition of geopolymer mortars (wt%)

Mix	O	C	Si	Na	K	Ca	Al	Mg	P	Fe	Mn	Si/Al	Si/Ca	Ca/Al
CT	41.2	27.9	14.1	6.7	3.2	2.2	1.5	1.4	1.1	0.8	-	9.4	6.41	1.5
5A	48.9	19.6	8.5	13.1	2.0	5.5	1.5	0.9	0.6	0.4	-	5.7	1.54	3.7
10A	48.0	16.3	5.9	16.0	1.4	9.7	1.2	0.7	0.4	0.3	-	4.9	0.61	8.1
1L	50.2	3.7	12.5	8.5	4.2	7.5	-	7.3	4.8	0.3	0.9	-	1.67	-
10L	52.0	16.7	9.7	15.8	2.1	1.1	0.6	1.0	0.5	0.4		16.2	8.82	1.8

4. Conclusions

This investigation evaluated the effect of alumina powder and field Para rubber latex incorporation on the compressive strength, bulk density, water absorption, and microstructural analysis of POA-based geopolymer binders. From the experimental results, the main conclusions are presented below:

- Alumina powder can improve the compressive strength of geopolymer from POA. The highest compressive strengths were developed by geopolymer mortars containing 5% AP for curing at ambient temperature, as well as with bulk density and water absorption of 1,867 kg/m^3 and 2.05%, respectively, after 28 days of curing.

- The compressive strength was highly developed with partial replacement at 5% AP content in comparison with the CT sample at 1 day and 28 days. The compressive strengths of 5% AP specimens were 5.19 MPa and 28.16 MPa, against 3.62 MPa and 18.86 MPa for the CT sample.

- Geopolymer from POA can use 1% FPRL to improve the compressive strength under curing at ambient temperature conditions.

- Using the AP combination of geopolymer matrix had a slight effect on the compressive strength when using FPRL at 1-5%.

- Using AP and FPRL in POA geopolymer increased the bulk density under POC aggregate.

- Microstructure images demonstrate the good reaction extent in the 5A sample with the density and compactness of the gel.

- Energy-dispersive X-ray spectroscopy showed enhanced formation of N-A-S-H in AP incorporated mixes. The increased compressive strength was attributable to the structure of the geopolymer matrix, which had a dense-compact structure and contained fewer unreacted raw materials. The increase in AP or FPRL reduced the Si content of the geopolymer binder system.

5. Declarations

5.1. Author Contributions

Conceptualization, A.H.; methodology, A.H., P.S., A.A., and K.O.; formal analysis, A.H.; investigation, A.H.; resources, A.H. and K.O.; writing—original draft preparation, A.H.; writing—review and editing, A.A. and W.P.; supervision, A.H. and P.S.; project administration, A.H. All authors have read and agreed to the published version of the manuscript.

6. References

[1] Juenger, M. C. G., Winnefeld, F., Provis, J. L., & Ideker, J. H. (2011). Advances in alternative cementitious binders. Cement and Concrete Research, 41(12), 1232–1243. doi:10.1016/j.cemconres.2010.11.012.

[2] Hawa, A., & Prachasaree, W. (2020). The development of compressive strength, drying shrinkage and microstructure of fly ash geopolymer with field para rubber latex. Revista Romana de Materiale/ Romanian Journal of Materials, 50(1), 59–68.

[3] Bhavsar, J. K., & Panchal, V. (2022). Ceramic Waste Powder as a Partial Substitute of Fly Ash for Geopolymer Concrete Cured at Ambient Temperature. Civil Engineering Journal (Iran), 8(7), 1369–1387. doi:10.28991/CEJ-2022-08-07-05.

[4] Ge, X., Hu, X., & Shi, C. (2022). Impact of micro characteristics on the formation of high-strength Class F fly ash-based geopolymers cured at ambient conditions. Construction and Building Materials, 352, 129074. doi:10.1016/j.conbuildmat.2022.129074.

[5] Aziz, I. H., Abdullah, M. M. A. B., Mohd Salleh, M. A. A., Azimi, E. A., Chaiprapa, J., & Sandu, A. V. (2020). Strength development of solely ground granulated blast furnace slag geopolymers. Construction and Building Materials, 250, 118720. doi:10.1016/j.conbuildmat.2020.118720.

[6] Nistratov, A. V., Klimenko, N. N., Pustynnikov, I. V., & Vu, L. K. (2022). Thermal Regeneration and Reuse of Carbon and Glass Fibers from Waste Composites. Emerging Science Journal, 6(5), 967-984. doi:10.28991/ESJ-2022-06-05-04.

[7] Hawa, A., Prachasaree, W., & Tonnayopas, D. (2017). Effect of water-to-powder ratios on the compressive strength and microstructure of metakaolin based geopolymers. Indian Journal of Engineering and Materials Sciences, 24(6), 499–506.

[8] Trincal, V., Multon, S., Benavent, V., Lahalle, H., Balsamo, B., Caron, A., Bucher, R., Diaz Caselles, L., & Cyr, M. (2022). Shrinkage mitigation of metakaolin-based geopolymer activated by sodium silicate solution. Cement and Concrete Research, 162, 106993. doi:10.1016/j.cemconres.2022.106993.

[9] Allaoui, D., Nadi, M., Hattani, F., Majdoubi, H., Haddaji, Y., Mansouri, S., Oumam, M., Hannache, H., & Manoun, B. (2022). Eco-friendly geopolymer concrete based on metakaolin and ceramics sanitaryware wastes. Ceramics International, 48(23), 34793–34802. doi:10.1016/j.ceramint.2022.08.068.

[10] Safari, Z., Kurda, R., Al-Hadad, B., Mahmood, F., & Tapan, M. (2020). Mechanical characteristics of pumice-based geopolymer paste. Resources, Conservation and Recycling, 162, 105055. doi:10.1016/j.resconrec.2020.105055.

[11] Hamid, M. A., Yaltay, N., & Türkmenoğlu, M. (2022). Properties of pumice-fly ash based geopolymer paste. Construction and Building Materials, 316, 125665. doi:10.1016/j.conbuildmat.2021.125665.

[12] Gao, Y., Guo, T., Li, Z., Zhou, Z., & Zhang, J. (2022). Mechanism of retarder on hydration process and mechanical properties of red mud-based geopolymer cementitious materials. Construction and Building Materials, 356, 129306. doi:10.1016/j.conbuildmat.2022.129306.

[13] Sun, Z., Tang, Q., Xakalashe, B. S., Fan, X., Gan, M., Chen, X., Ji, Z., Huang, X., & Friedrich, B. (2022). Mechanical and environmental characteristics of red mud geopolymers. Construction and Building Materials, 321, 125564. doi:10.1016/j.conbuildmat.2021.125564.

[14] Ranjbar, N., Mehrali, M., Behnia, A., Alengaram, U. J., & Jumaat, M. Z. (2014). Compressive strength and microstructural analysis of fly ash/palm oil fuel ash based geopolymer mortar. Materials & Design, 59, 532-539. doi:10.1016/j.matdes.2014.03.037.

[15] Abdulkareem, O. A., Ramli, M., & Matthews, J. C. (2019). Production of geopolymer mortar system containing high calcium biomass wood ash as a partial substitution to fly ash: An early age evaluation. Composites Part B: Engineering, 174, 106941. doi:10.1016/j.compositesb.2019.106941.

[16] Somna, R., Saowapun, T., Somna, K., & Chindaprasirt, P. (2022). Rice husk ash and fly ash geopolymer hollow block based on NaOH activated. Case Studies in Construction Materials, 16, 1092. doi:10.1016/j.cscm.2022.e01092.

[17] Islam, A., Alengaram, U. J., Jumaat, M. Z., Bashar, I. I., & Kabir, S. M. A. (2015). Engineering properties and carbon footprint of ground granulated blast-furnace slag-palm oil fuel ash-based structural geopolymer concrete. Construction and Building Materials, 101(1), 503–521. doi:10.1016/j.conbuildmat.2015.10.026.

[18] Hawa, A., Tonnayopas, D., Prachasaree, W., & Taneerananon, P. (2013). Investigating the effects of oil palm ash in metakaolin based geopolymer. Ceramics-Silikaty, 57(4), 319-327.

[19] Hawa, A., Tonnayopas, D., & Prachasaree, W. (2014). Performance Evaluation of Metakaolin Based Geopolymer Containing Parawood Ash and Oil Palm Ash Blends. Materials Science, 20(3), 339–344. doi:10.5755/j01.ms.20.3.4543.

[20] Liu, X., Jiang, J., Zhang, H., Li, M., Wu, Y., Guo, L., Wang, W., Duan, P., Zhang, W., & Zhang, Z. (2020). Thermal stability and microstructure of metakaolin-based geopolymer blended with rice husk ash. Applied Clay Science, 196, 105769. doi:10.1016/j.clay.2020.105769.

[21] Rukzon, S., & Chindaprasirt, P. (2009). Use of disposed waste ash from landfills to replace Portland cement. Waste Management & Research, 27(6), 588-594. doi:10.1177/0734242X09103189.

[22] Liu, M. Y. J., Alengaram, U. J., Santhanam, M., Jumaat, M. Z., & Mo, K. H. (2016). Microstructural investigations of palm oil fuel ash and fly ash based binders in lightweight aggregate foamed geopolymer concrete. Construction and Building Materials, 120, 112–122. doi:10.1016/j.conbuildmat.2016.05.076.

[23] Zarina, Y., Mustafa Al Bakri, A. M., Kamarudin, H., Nizar, I. K., & Rafiza, A. R. (2013). Review on the various ash from palm oil waste as geopolymer material. Reviews on Advanced Materials Science, 34(1), 37–43.

[24] Amri, A., Fathurrahman, G., Najib, A. A., Awaltanova, E., Aman, & Chairul. (2018). Composites of palm oil fuel ash (POFA) based geopolymer and graphene oxide: Structural and compressive strength. IOP Conference Series: Materials Science and Engineering, 420(1), 12063. doi:10.1088/1757-899X/420/1/012063.

[25] Rattanasak, U., Chindaprasirt, P., & Suwanvitaya, P. (2010). Development of high volume rice husk ash alumino silicate composites. International Journal of Minerals, Metallurgy and Materials, 17(5), 654–659. doi:10.1007/s12613-010-0370-0.

[26] Mijarsh, M. J. A., Megat Johari, M. A., & Ahmad, Z. A. (2014). Synthesis of geopolymer from large amounts of treated palm oil fuel ash: Application of the Taguchi method in investigating the main parameters affecting compressive strength. Construction and Building Materials, 52, 473–481. doi:10.1016/j.conbuildmat.2013.11.039.

[27] Darvish, P., Johnson Alengaram, U., Soon Poh, Y., Ibrahim, S., & Yusoff, S. (2020). Performance evaluation of palm oil clinker sand as replacement for conventional sand in geopolymer mortar. Construction and Building Materials, 258, 120352. doi:10.1016/j.conbuildmat.2020.120352.

[28] Ong, E. L. (1998). Latex protein allergy and your gloves/Ong Eng Long, Esah Yip and Lai Pin Fah. Malaysian Rubber Board, Kuala Lumpur, Malaysia.

[29] Rubber Authority of Thailand. (2017). knowledge of latex and constituents in latex. Rubber Authority of Thailand, Bangkok, Thailand. Available online: https://km.raot.co.th/km-knowledge/detail/259 (accessed on April 2023).

[30] Office of Agricultural Economics. (2020). Para rubber: percentage and monthly output Including countries, regions and provinces. Office of Agricultural Economics, Bangkok, Thailand, Available online: https://www.oae.go.th/assets/portals/1/fileups/prcaidata/files/pencent%2063.pdf (accessed on April 2023).

[31] Yaowarat, T., Suddeepong, A., Hoy, M., Horpibulsuk, S., Takaikaew, T., Vichitcholchai, N., Arulrajah, A., & Chinkulkijniwat, A. (2021). Improvement of flexural strength of concrete pavements using natural rubber latex. Construction and Building Materials, 282, 122704. doi:10.1016/j.conbuildmat.2021.122704.

[32] Kabir, S. M. A., Alengaram, U. J., Jumaat, M. Z., Yusoff, S., Sharmin, A., & Bashar, I. I. (2017). Performance evaluation and some durability characteristics of environmental friendly palm oil clinker based geopolymer concrete. Journal of Cleaner Production, 161, 477–492. doi:10.1016/j.jclepro.2017.05.002.

[33] Chandara, C., Sakai, E., Azizli, K. A. M., Ahmad, Z. A., & Hashim, S. F. S. (2010). The effect of unburned carbon in palm oil fuel ash on fluidity of cement pastes containing superplasticizer. Construction and Building Materials, 24(9), 1590–1593. doi:10.1016/j.conbuildmat.2010.02.036.

[34] ASTM C136/C136M-19. (2019). Standard Test Method for Sieve Analysis of Fine and Coarse Aggregates. ASTM international, Pennsylvania, United States. doi:10.1520/C0136_C0136M-19.

[35] ASTM C33/C33M-18. (2018). Standard Specification for Concrete Aggregates. ASTM international, Pennsylvania, United States. doi:10.1520/C0033_C0033M-18.

[36] Hawa, A., Tonnayopas, D., & Prachasaree, W. (2013). Performance evaluation and microstructure characterization of metakaolin-based geopolymer containing oil palm ash. The Scientific World Journal, 2013, 857586. doi:10.1155/2013/857586.

[37] ASTM C109/C109M-16a. (2016). Standard Test Method for Compressive Strength of Hydraulic Cement Mortars (Using 2-in. or [50-mm] Cube Specimens). ASTM international, Pennsylvania, United States.

[38] Ranjbar, N., Mehrali, M., Behnia, A., Alengaram, U. J., & Jumaat, M. Z. (2014). Compressive strength and microstructural analysis of fly ash/palm oil fuel ash based geopolymer mortar. Materials and Design, 59, 532–539. doi:10.1016/j.matdes.2014.03.037.

[39] Islam, A., Alengaram, U. J., Jumaat, M. Z., & Bashar, I. I. (2014). The development of compressive strength of ground granulated blast furnace slag-palm oil fuel ash-fly ash based geopolymer mortar. Materials and Design, 56, 833–841. doi:10.1016/j.matdes.2013.11.080.

[40] Silva, P. De, Sagoe-Crenstil, K., & Sirivivatnanon, V. (2007). Kinetics of geopolymerization: Role of Al2O3 and SiO2. Cement and Concrete Research, 37(4), 512–518. doi:10.1016/j.cemconres.2007.01.003.

[41] Kwek, S. Y., Awang, H., & Cheah, C. B. (2021). Influence of liquid-to-solid and alkaline activator (Sodium silicate to sodium hydroxide) ratios on fresh and hardened properties of alkali-activated palm oil fuel ash geopolymer. Materials, 14(15), 4253. doi:10.3390/ma14154253.

[42] Salih, M. A., Abang Ali, A. A., & Farzadnia, N. (2014). Characterization of mechanical and microstructural properties of palm oil fuel ash geopolymer cement paste. Construction and Building Materials, 65, 592–603. doi:10.1016/j.conbuildmat.2014.05.031.

[43] Hawa, A., Salaemae, P., Prachasaree, W., & Tonnayopas, D. (2017). Compressive strength and microstructural characteristics of fly ash based geopolymer with high volume field para rubber latex. Revista Romana de Materiale/ Romanian Journal of Materials, 47(4), 462–469.

[44] Rath, B., Debnath, R., Paul, A., Velusamy, P., & Balamoorthy, D. (2020). Performance of natural rubber latex on calcined clay-based glass fiber-reinforced geopolymer concrete. Asian Journal of Civil Engineering, 21(6), 1051–1066. doi:10.1007/s42107-020-00261-z.

[45] Rath, B. (2022). Effect of natural rubber latex on the shrinkage behavior and porosity of geopolymer concrete. Structural Concrete, 23(4), 2150–2161. doi:10.1002/suco.202000788.

[46] Kourti, I., Rani, D. A., Deegan, D., Boccaccini, A. R., & Cheeseman, C. R. (2010). Production of geopolymers using glass produced from DC plasma treatment of air pollution control (APC) residues. Journal of Hazardous Materials, 176(1–3), 704–709. doi:10.1016/j.jhazmat.2009.11.089.

[47] He, P., Wang, M., Fu, S., Jia, D., Yan, S., Yuan, J., Xu, J., Wang, P., & Zhou, Y. (2016). Effects of Si/Al ratio on the structure and properties of metakaolin based geopolymer. Ceramics International, 42(13), 14416–14422. doi:10.1016/j.ceramint.2016.06.033.

[48] Ariffin, M. A. M., Bhutta, M. A. R., Hussin, M. W., Mohd Tahir, M., & Aziah, N. (2013). Sulfuric acid resistance of blended ash geopolymer concrete. Construction and Building Materials, 43, 80–86. doi:10.1016/j.conbuildmat.2013.01.018.

[49] Puertas, F., Palacios, M., Manzano, H., Dolado, J. S., Rico, A., & Rodríguez, J. (2011). A model for the C-A-S-H gel formed in alkali-activated slag cements. Journal of the European Ceramic Society, 31(12), 2043–2056. doi:10.1016/j.jeurceramsoc.2011.04.036.

[50] Salih, M. A., Farzadnia, N., Abang Ali, A. A., & Demirboga, R. (2015). Development of high strength alkali activated binder using palm oil fuel ash and GGBS at ambient temperature. Construction and Building Materials, 93, 289–300. doi:10.1016/j.conbuildmat.2015.05.119.

[51] Walkley, B., Provis, J. L., San Nicolas, R., Sani, M. A., & Van Deventer, J. S. J. (2015). Stoichiometrically controlled C-(A)-S-H/N-A-S-H gel blends via alkali activation of synthetic precursors. Advances in Applied Ceramics, 114(7), 372–377. doi:10.1179/1743676115Y.0000000057.

[52] Li, W., Wang, Y., Yu, C., He, Z., Zuo, C., & Yu, Y. (2023). Nano-scale study on molecular structure, thermal stability, and mechanical properties of geopolymer. Journal of the Korean Ceramic Society, 60(2), 413–423. doi:10.1007/s43207-022-00276-z.